Hindawi
Shock and Vibration
Volume 2021, Article ID 2280348, 11 pages
https://doi.org/10.1155/2021/2280348

Research Article

Experiment and Mechanism Investigation on Freezing-Thawing of Sandstone with Different Water Contents

Guilei Song,[1] **Longxiao Chen**,[1] **Kesheng Li**,[2] **Deng Zhang**,[3] **Junhao Xu**,[1] **Wenshuo Xu**,[1] **Chuanxiao Liu**,[1] **and Jinpeng Zhang**[1]

[1]*College of Water Conservancy and Civil Engineering, Shandong Agricultural University, Tai'an 271018, Shandong, China*
[2]*State Key Laboratory for Geomechanics and Deep Underground Engineering, China University of Mining and Technology, Xuzhou, Jiangsu 221116, China*
[3]*School of Civil Engineering, Qingdao University of Technology, Qingdao 266033, China*

Correspondence should be addressed to Chuanxiao Liu; lchuanx@163.com and Jinpeng Zhang; zjpsdust@126.com

Received 5 September 2021; Accepted 9 October 2021; Published 15 November 2021

Academic Editor: Xiao Wang

Freezing-thawing cycles seriously affect the safety of underground engineering in cold regions. At present, most research studies focus on the effect of number and freezing temperature on freezing-thawing cycles. As another important factor, the mechanism of rock mass water content affecting freezing-thawing is less studied. This paper studied the influence of the water content on mechanical property, microstructure, and acoustic emission characteristics of sandstone. The results indicated that the uniaxial compressive strength (UCS) and elastic modulus (E) of sandstone after 20 freezing-thawing cycles decreased as the water content increased. However, the decreasing rate of UCS gradually decreased, while the decreasing rate of E gradually increased. Furthermore, the empirical formulas of UCS and E about water content were obtained. The porosity and plasticity of sandstone after 20 freezing-thawing cycles increased as the water content increased. The empirical formulas of UCS and E about water content were obtained. The porosity and plasticity of sandstone after 20 freezing-thawing cycles increased as the water content increased. The decreasing trend of UCS with porosity was the same as that of UCS with water content. The failure form of sandstone gradually changed from splitting failure to shear failure. The results of the acoustic emission test showed that the stress-strain curves combined with acoustic emission ring counting could reveal the damage evolution process of sandstone during loading.

1. Introduction

In cold regions such as northern China, northwestern Iran, and eastern Turkey, the effects of freezing and thawing are experienced every year, which bring huge challenges to local underground engineering. Rock mass is a kind of natural mineral aggregate, containing certain cracks, pores, gas, water, etc. The temperature change will cause the pore water in rock mass to continuously undergo water-ice phase transition. The frost heaving force caused by volume expansion makes the primary cracks and pores in rock develop continuously, fuse and connect, and then generate new cracks, which destroy the internal microstructure of rock and lead to the continuous deterioration of rock properties [1, 2]. Thus, freezing-thawing is a primary reason for the deterioration of rock properties.

Previous research studies have generally shown that freezing-thawing process significantly affects the mechanical parameters of rocks. Mousavi et al. investigated the effect of the freezing-thawing cycles on the mechanical properties of schists and showed that the uniaxial compressive strength (UCS), elastic modulus (E), cohesive force, and internal friction angle were decreased exponentially by increasing the number of freezing-thawing cycles [3, 4]. Jia et al. and Liu et al. investigated the evolution law of frost heaving force of cracks containing ice under freezing-thawing cycles and

then revealed the effect mechanism of fatigue freeze-thaw on rock mass structure deterioration [5, 6]. Su et al. and Wang et al. investigated the damage mechanism of rock under freezing-thawing cycles using acoustic emission monitoring technology [7, 8]. Jiang and Zhou et al. revealed the relationship between mechanical properties and microstructure degradation of rock after freezing-thawing cycles [9, 10]. Chen et al. studied the changes in sandstone porosity after freezing-thawing cycles under low confining pressure by mercury intrusion measurement technology and found that the freezing-thawing cycles would greatly increase the large pores and super-large pores in the rock, thereby reducing mechanical properties of rock [11].

On the other hand, some scholars have deeply explored its mechanical mechanism by establishing the damage constitutive equation of freeze-thaw stone. Huang et al. deduced the damage constitutive equation of freeze-thaw sandstone under load, which was established based on the assumption that the microunit strength satisfies the Weibull distribution and the maximum-tensile-strain yield criterion [12]. Based on the Lemaitre strain equivalent principle and continuum damage mechanics theory, Lu et al. deduced the damage constitutive equation under freezing-thawing cycles and loading, in which pre-existing cracks, confining pressure, freeze-thaw action, and load were considered, and established the damage model to predict the degradation of triaxial compression strength for single flaw sandstone [13]. These studies had important implications for engineering safety in cold regions. Also, there are many factors that affect the effects of freezing-thawing cycles [14], such as the number and the temperature of freezing-thawing cycles and the hydration conditions during freezing-thawing [15–17]. Water content is also one of the most important factors.

Existing studies generally showed that the mechanical properties of rock such as cohesive force, internal friction angle, and uniaxial and triaxial compressive strength decrease with the increase of water content [18–20]. By analyzing the failure characteristics of rocks with different water contents, the researchers found that the increase of water content would increase the total strain of rock, reduce the brittleness, and increase the damage degree [21]. Chen et al. found that when the water content exceeded the critical saturation, the mechanical properties of red sandstone changed significantly and further obtained a model that can predict the damage of red sandstone with different water-bearing states undergoing freezing-thawing cycles [22]. Liu et al. found that the deterioration degree of red sandstone increased rapidly with the increase of freezing-thawing cycle times when the saturation was greater than the critical saturation of 60% [23]. Omari and Walbert et al. found that the critical saturation of rock was not a definite value [24, 25]. Fan et al. studied the effect of mechanical properties of rock with different water-bearing states and proposed the empirical equation of sandstone mechanical behavior [26]. Weng et al. studied the dynamic mechanical properties of rock with different water contents after freeze-thaw cycles [27]. Therefore, water content is an important factor that affects the mechanical properties of rocks. Most of the previous studies which investigated the influence of water content on rock mechanical properties did not consider the freeze-thaw effect. However, rock mass is not saturated and experiences freezing-thawing cycles in the natural state of cold areas. Thus, it is more meaningful to consider the freezing-thawing cycles when studying the effect of different water content on sandstone.

The research investigated the mechanical properties, microstructure, and acoustic emission characteristics of sandstone with different water contents of 0%, 0.58%, 1.06%, 1.82%, 2.43%, and 2.80% under 20 freezing-thawing cycles. The test used 20 freezing-thawing cycles to simulate the freezing-thawing cycles experienced by the actual project during the service life. The influences of the water content on deformation and strength characteristics, pore characteristics, and AE ring count of the sandstone under the freezing-thawing cycles were discussed. The research aims to explore how the bearing capacity of tunnel surrounding rock with different water contents changes after several freezing-thawing cycles in cold areas and provide information and suggestions for the maintenance of the tunnel project during its use period.

2. Materials and Methods

2.1. Sample Preparation. The sandstone was taken from a tunnel engineering in the cold northern part of China. In the laboratory, the large sandstone was made into the cylindrical sample of Φ50◊100 mm through the automatic stone cutter, the core drilling machine, and the double end automatic grinding machine (Figure 1). The rock that did not conform to the test specifications, such as macroscopic, stratification, or significant differences, was excluded.

In order to research the influence of moisture content on the mechanical properties and acoustic emission characteristics of sandstone, the sandstone was divided into six groups. Every group included 3 sandstone samples. To obtain sandstone with different water contents, firstly three samples were placed in a dry oven at 105°C to 110°C for 24 hours, then cooled to room temperature, and finally soaked in water until they were saturated. The sandstone was taken out from water and weighed every 30 minutes. The curve of water content and soaking time of sandstone is shown in Figure 2. It could be seen from Figure 2 that the relationship between moisture content and soaking time could be divided into four stages including the rapid growth stage (I), the stable growth stage (II), the deceleration growth stage (III), and the stable water-bearing stage (IV). In order to make the test more rigorous, as many test variables as possible should be selected, so six different moisture contents were selected for this test. In order to make the six kinds of moisture content as evenly distributed as possible and representative, one or two representative soaking times at each stage were chosen to soak the samples to obtain different water content. Then, the average water content of each group of specimens was selected as the final water content. In the test, the sandstone after drying were soaked for 0 min, 30 min, 60 min, 390 min, 900 min, and 1500 min, respectively [28]. The empirical formulas between moisture content and

(a) (b) (c)

Figure 1: (a) SCQ type automatic stone cutter. (b) Core drilling machine. (c) Double end automatic grinding machine.

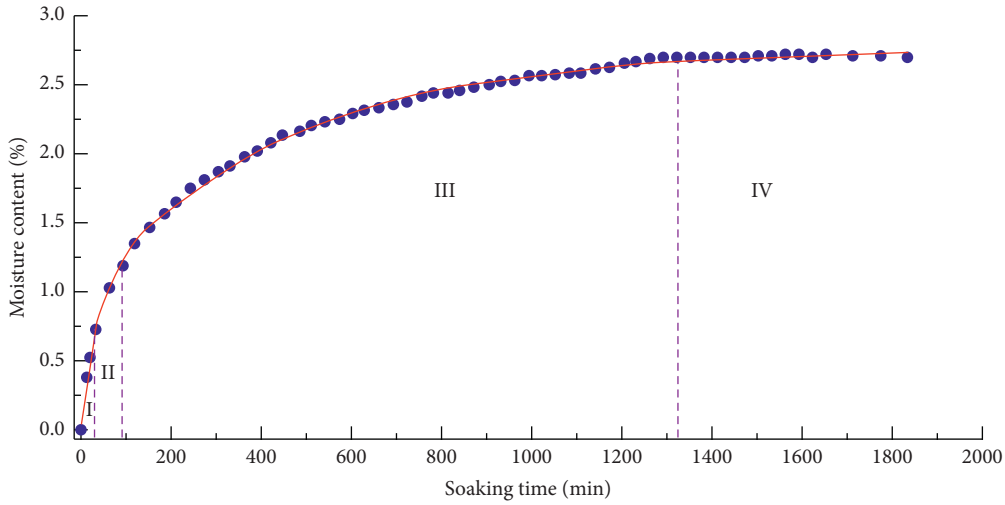

Figure 2: Fitting curve of the water content of sandstone and soaking time.

soaking time were obtained, as shown in the following equation:

$$\omega = 0.042 + 0.938\left(1 - e^{-0.03t}\right) + 1.778\left(1 - e^{-0.002t}\right), \quad R^2 = 0.99868, \tag{1}$$

where ω is the water content and t is the soaking time.

Firstly, all specimens were dried in the temperature of 105–110°C for 48 hours and then transferred to the dryer and weighed. One group of rock samples after drying was used as standard sample with water content of 0%. The remaining five groups of sandstone were, respectively, soaked into water for 30 min, 60 min, 390 min, 900 min, and 1500 min. After that, the rock samples were taken out, wiped off the surface water, and weighed. The samples with water content of 0.58%, 1.06%, 1.82%, 2.43%, and 2.80% were obtained, as shown in Table 1. A typical sample was selected from each group for analysis.

Table 1: Relationship between water content of sandstone and soaking time.

Serial number	WT1	WT2	WT3	WT4	WT5	WT6
Soaking time (min)	0	30	60	390	900	1500
Water content (%)	0	0.58	1.06	1.82	2.43	2.80

2.2. Experimental Design

2.2.1. Freeze-Thaw Test. The specimens were frozen and thawed to better simulate the environment in North China. Hence, the specimens firstly were wrapped tightly with plastic wrap and put in a freezer with a temperature of −20°C for 4 hours. Finally, all specimens were moved to a constant water temperature of +20°C for 4 hours according to previous test methods [29]. This meant that each freezing-thawing cycle required about 8 hours. Furthermore, we studied mainly the effect of water content on the mechanism investigation of sandstone under freezing-thawing cycles. Therefore, freezing-thawing cycles times were selected to be 20 according to the corresponding test specification [30].

2.2.2. Uniaxial Compression Test. The conventional uniaxial compression test was performed on six groups of sandstone with different water contents using Saw-2000 microcomputer-controlled electrohydraulic servo rock triaxial pressure testing machine (Figure 3(a)). The electrohydraulic

(a) (b)

Figure 3: Test equipment. (a) Saw-2000 microcomputer-controlled electrohydraulic servo rock triaxial pressure testing machine. (b) AW21C acoustic emission detector.

servo displacement control method with the displacement rate of 0.002 mm/s was adopted to load the rock sample. The AW21C acoustic emission detector (Figure 3(b)) was used to detect acoustic emission signals during the loading process. The test parameters of the instrument were set, including sampling frequency of 10 MHz, gain of 30 dB, threshold value of 35 dB, impact definition time of 50 μs, impact interval time of 300 μs, and adjusting threshold voltage of 1.0 V.

3. Mechanical Property Analysis

3.1. Stress-Strain Curve Analysis. The stress-strain curves obtained by the uniaxial compression test were firstly studied as shown in Figure 4. The stress-strain curves were roughly divided into four typical stages, specifically the initial compaction stage, the elastic deformation stage, the plastic deformation stage, and the failure stage.

At the initial compaction stage, the stress-strain curves showed a nonlinear concave shape, where the nonlinear deformation increased as the water content increased. This indicated that the higher the moisture content of sandstone, the higher the porosity. After 20 freezing-thawing cycles, the original cracks of all sandstones were constantly damaged and bred into new cracks under the effect of water-rock action and frost heaving pressure. The higher the water content, the higher the porosity, which also led to the greater deformation of the sandstone at this stage. At the elastic deformation stage, the relationship between stress and strain was linear. The slope of the straight line decreased as the water content increased. It meant that the elastic modulus decreased as the water content increased. At the plastic deformation stage, an increasing number of microfractures were generated as the load increased, causing the samples to gradually enter an unstable state. Finally, the microfractures were transferred to macrofractures. The plastic deformation rate was gradually accelerated at this stage. When the maximum stress was reached, the specimen failed. At the failure stage, the stress decreased rapidly.

3.2. UCS Analysis. In this section, UCS of the sandstones with different moisture content was studied. The results showed that the UCS of sandstone decreased as the moisture content increased. The rate of decrease gradually reduced, indicating that the deterioration rate of sandstone decreased. Moreover, the decrease rate of UCS was the fastest at the early stage as the water content increased. The UCS decreased by 12.99% from 82.39 MPa to 71.69 MPa when the water content increased by 0.58% from 0 [28]. The UCS decreased by 37.31% when the water content increased by 2.80% from 0.

Coefficient (R^2) was used to characterize the correlation between the fitting formula and the original data. The closer R^2 was to 1, the better the fitting effect. The exponential function produces the highest R in the linear, exponential, and polynomial fitting relationships (Table 2), so it was used to describe the relationship between UCS and water content (Figure 5). The function is shown in the following equation:

$$\mathrm{UCS}(\omega) = 42.84 + 38.79 \times 0.63^{\omega}. \quad (2)$$

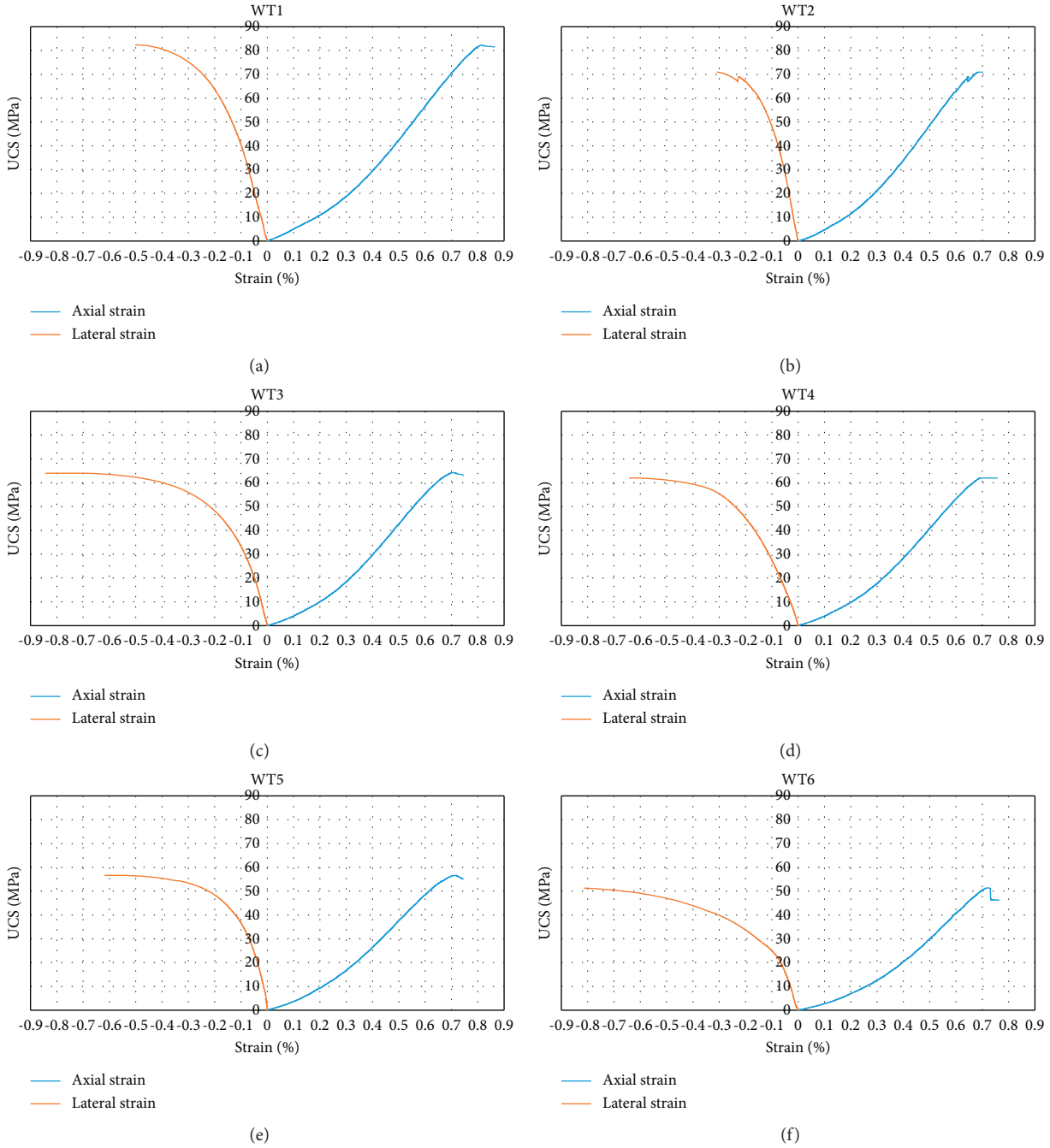

Figure 4: The stress-strain curves of sandstone with diffident water contents.

Table 2: The function and R^2 used to fit UCS and ω.

Fitting function	R^2
Polynomial fit	0.96945
Linear fit	0.95134
Exponential fit	0.97439

3.3. Elastic Modulus Analysis. The fitting curve of elastic modulus (E) is demonstrated in Figure 6. It could be seen that the value of E also decreased as the water content increased. However, the decrease rate of E was gradually increasing, which was different from UCS. E decreased by 7.6% from 11.21 GPa to 10.33 GPa when the water content increased by 2.80% from 2.43%. E decreased by 25.05% from 13.78 GPa to 10.33 GPa when the water content increased by 2.80% from 0. E of the sandstone with the water content of 2.80% decreased by 25.05% compared with sandstone with 0 water content.

In this section, R^2 of various fitting equations is shown in Table 3. It could be seen that R^2 of the polynomial fitting curve was the highest, 0.98509, so the polynomial equation was used to fit the relationship between E and ω. As a result, the polynomial function was expressed by

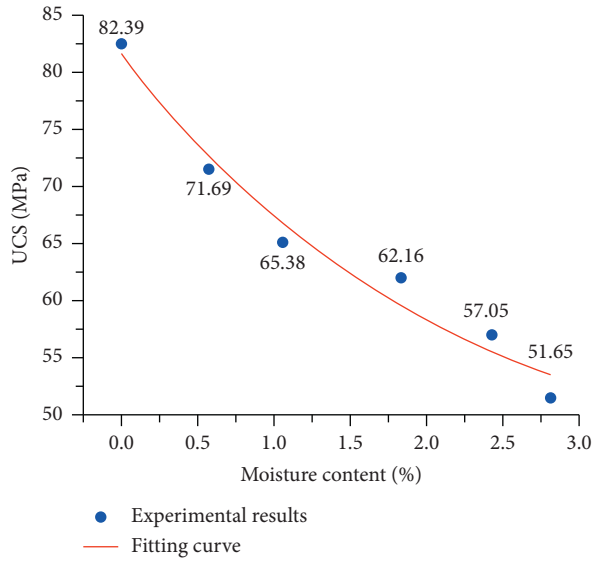

Figure 5: Relationship between UCS and ω.

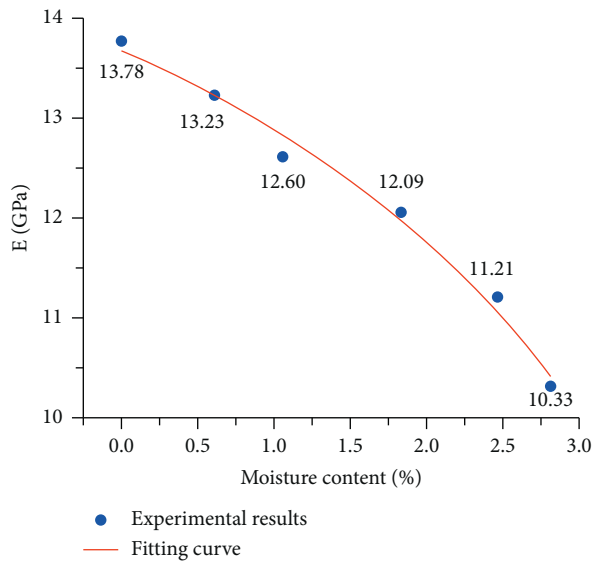

Figure 6: Relationship between E and ω.

Table 3: The function and R^2 used to fit E and ω.

Fitting function	R^2
Polynomial fit	0.98622
Linear fit	0.97206
Exponential fit	0.97201

$$E(\omega) = -0.177\omega^2 - 0.653\omega + 13.697. \quad (3)$$

3.4. Mechanism Analysis. Figure 7 shows the scanning electron microscopy (SEM) images of sandstone with different moisture contents under 20 freezing-thawing cycles. It could be seen that the number of micropores and microcracks in samples was increasing with the increase of moisture content. In order to obtain the relationship between moisture content and porosity more accurately, the SEM images were binarized by ImageJ software, as shown in Figure 8 and Table 4. Compared with the completely dry samples, the porosity of fully saturated sandstone increased significantly, from 3.56% to 10.36%. Then, the fitting curve of UCS and porosity was obtained, as shown in Figure 9. It could be seen that the decreasing trend of UCS with porosity was basically the same as that of UCS with moisture content. This was mainly manifested as water dissolving the cement between the particles, reducing the cohesive force and losing the internal structure. On the other hand, the volume expands by about 9% when the water-ice phase transition occurs, and the resulting frost heave pressure causes the continuous development of the original fractures in the samples, forming new fractures. So, the porosity of the sandstone increased after freezing-thawing cycles as the moisture content increased, which in turn reduced the mechanical properties. Through further analysis, the following reasons for sandstone destruction were obtained. The first reason was that the internal cementation and mineral ions were lost due to water-rock reaction, which reduced the internal compactness. Secondly, freezing-thawing cycles caused irregular deformation of sandstone internal structure, which led to fatigue damage of sandstone. Finally, holes and cracks appeared in the weak layers such as the interface and cementation inside the sandstone due to the frost swelling pressure caused by water freezing. Moreover, these damages continued to be developed and deteriorated, leading to the change of mechanical properties of sandstone [31].

4. Analysis of Failure Characteristics

The failure form of the sandstone with different water contents is shown in Figure 10. The failure modes of sandstone were mainly splitting failure and shear failure. The failure mode of sandstone with low water content was mainly splitting failure. These sandstones had high UCS and brittleness, so the applied load during uniaxial compression test was correspondingly higher, resulting in larger hoop stress. However, the tensile strength of sandstone was weak, and the failure form of sandstone was splitting failure due to the hoop stress. The failure form changed gradually to shear failure as the water content increased. Jiang et al. found through research that the lower the water content, the lower the plasticity of the rock. In other words, the plasticity of the rock increased gradually as the water content increased [32]. The cracks produced in the plastic deformation stage were mainly shear cracks [21], so the failure form of the sandstone was gradually transitioned to shear failure.

5. Analysis of Acoustic Emission Characteristics

Acoustic emission (AE) activities of rock are mainly caused by the generation, expansion, and fracture of cracks inside the rock and can reveal the damage of the rock [33]. The acoustic emission information of compressed rock contains

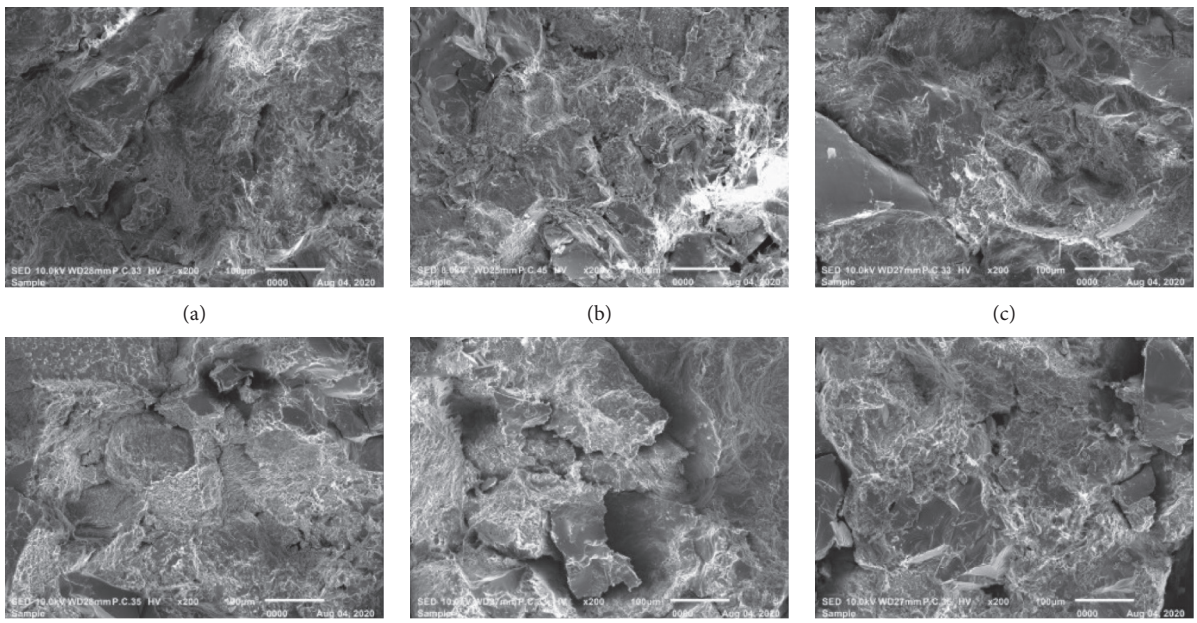

(a) (b) (c)

(d) (e) (f)

Figure 7: SEM images of sandstone with different water contents (magnifying 200 times). (a) $\omega = 0\%$. (b) $\omega = 0.57\%$. (c) $\omega = 1.06\%$. (d) $\omega = 1.82\%$. (e) $\omega = 2.43$. (f) $\omega = 2.80\%$.

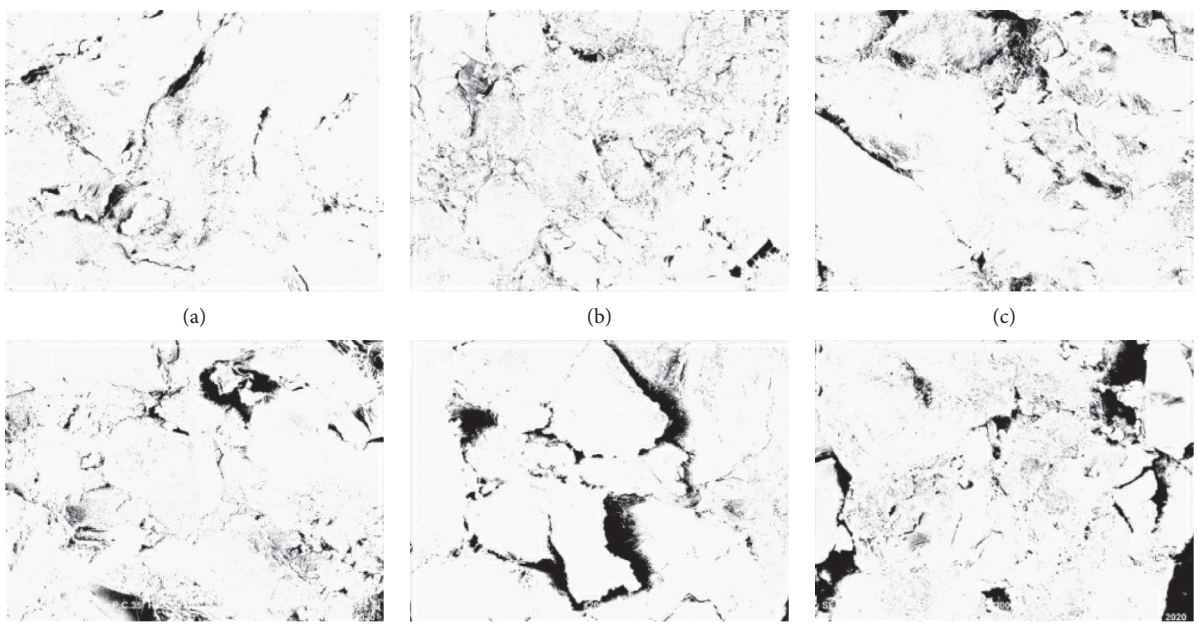

(a) (b) (c)

(d) (e) (f)

Figure 8: Binary images. (a) $\omega = 0\%$. (b) $\omega = 0.57\%$. (c) $\omega = 1.06\%$. (d) $\omega = 1.82\%$. (e) $\omega = 2.43$. (f) $\omega = 2.80\%$.

Table 4: Relationship between water content and porosity.

Water content (%)	0	0.58	1.06	1.82	2.43	2.80
Porosity (%)	3.56	4.95	6.54	6.77	8.23	10.36

abundant precursor information of rock failure, which is of great significance for predicting the damage process of rock [34].

The number of oscillations of the signal exceeding the threshold is named AE ringing count. The variation of ringing count-stress with time is shown in Figure 11. It could be seen that the ringing count of sandstone with different water content showed the same rule with time. At the initial stage of loading, specimens were in the initial compaction stage and elastic stage. The original cracks existing in the samples were compacted and closed. Elastic distortion

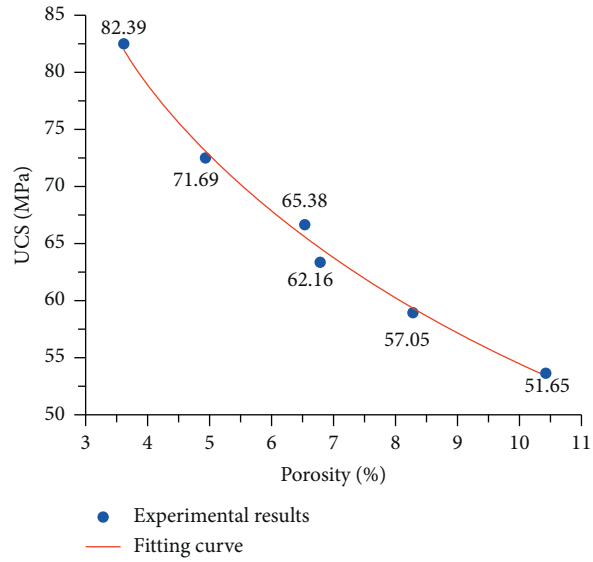

Figure 9: Relationship between UCS and porosity.

Figure 10: Failure form of sandstone with different water contents. (a) $\omega = 0\%$. (b) $\omega = 0.57\%$. (c) $\omega = 1.06\%$. (d) $\omega = 1.82\%$. (e) $\omega = 2.43$. (f) $\omega = 2.80\%$.

occurred in the sandstone, and fewer new cracks were generated, so there were fewer AE events. After entering the plastic deformation stage, the cracks began to produce, propagate, and break through. The elastic energy accumulated in the compaction stage and elastic stage could be released rapidly. AE events increase, and the ringing count was several times that of the previous two stages. As the loading continues, the cracks and pores in the specimen continued to expand and connect and then changed into macroscopic cracks. Eventually, the specimen was destroyed. AE events increased rapidly and the ringing count reached the maximum. It could be seen that before the failure of the specimen, the AE events have increased significantly, and when there was a stress drop, the AE events suddenly increased, which played an important role in predicting rock failure.

As the result, under the 20 freezing-thawing cycles, the ringing count did not show an obvious change rule as the water content increased. The reason for this phenomenon may be as follows: intergranular connection is weakened by hydration of clay minerals and water dissolution of soluble minerals within sandstone. Thus, the energy needed for sandstone specimen failure is reduced. As a result, acoustic emission activity and ringing count of sandstone should decrease with the increase of water content [22, 34–37]. In addition, freeze-thaw cycles can increase the acoustic emission activity of rocks in the loading stage [7, 8]. Moreover, under the same freezing-thawing cycle times, as the water content increased, the more obvious the freeze-thaw effect, the greater the damage inside the samples. The AE activity of sandstone should also be enhanced. Therefore, under the influence of freezing-thawing cycles and water content and different crack development of specimens themselves, the law of ringing count was not obvious.

6. Discussion

The cracks in the original rock seriously affect its mechanical properties, which in turn may affect the safety of the project. Obviously the greater the porosity of the rock, the worse its

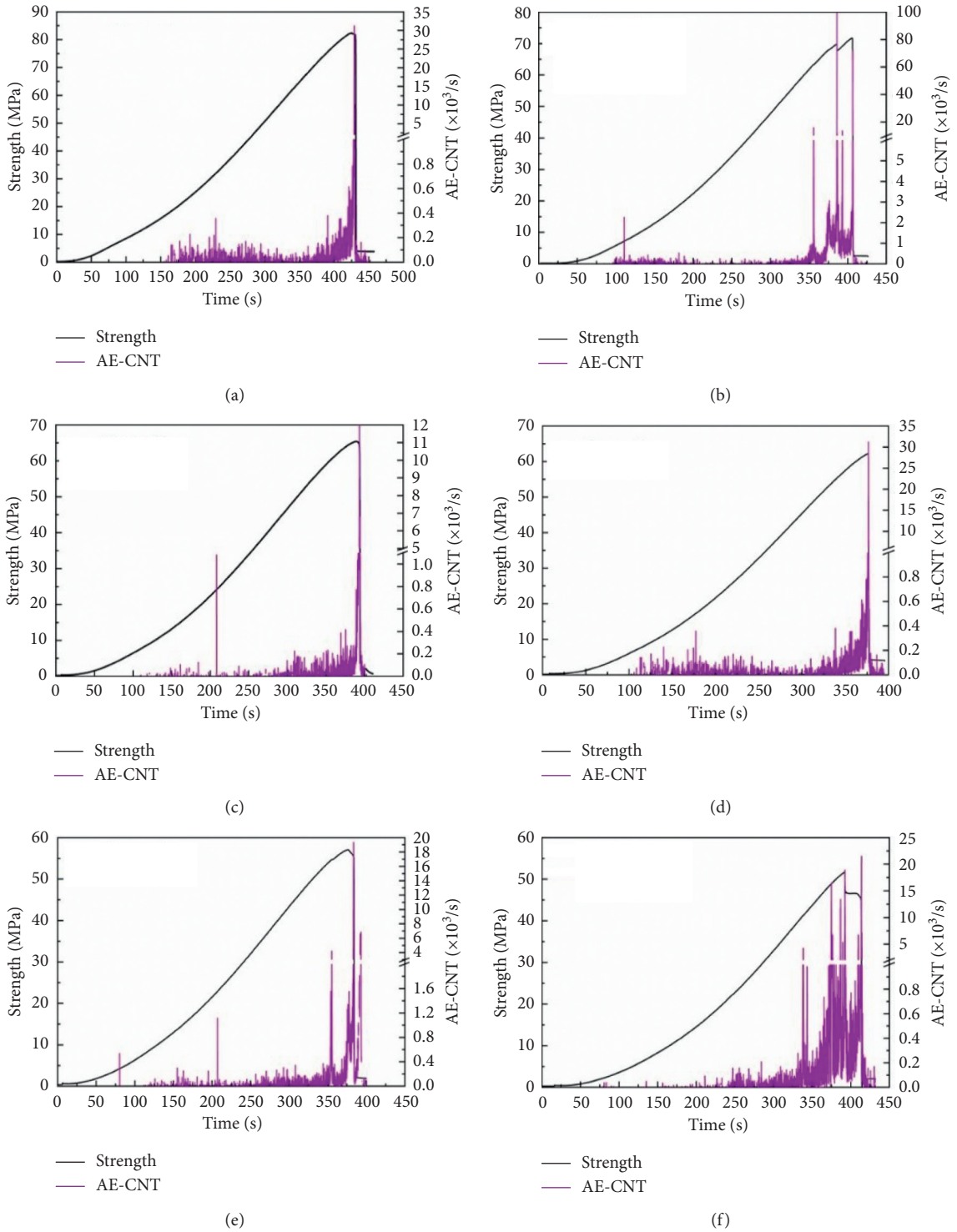

Figure 11: Relation of ringing count-stress with time. (a) $\omega = 0\%$. (b) $\omega = 0.57\%$. (c) $\omega = 1.06\%$. (d) $\omega = 1.82\%$. (e) $\omega = 2.43\%$. (f) $\omega = 2.80\%$.

bearing capacity. The water content has a significant impact on the porosity and mechanical properties of rock under the freezing-thawing cycles. In this study, the impact of different water contents on the mechanical properties and failure mechanism of sandstone after freezing-thawing cycles was investigated, providing information and suggestions for the engineering safety in cold regions.

Previous studies have shown that UCS of sandstone without the freezing-thawing cycle decreases linearly as the water content increased [18, 38, 39]. This was different from the experimental results of our experiment. The paper showed that when the water content was less than 1.06%, the UCS of sandstone had dropped substantially. Then, the declining rate of the UCS slowed down as the water content

continued to increase. The reason for this phenomenon may be that the freezing-thawing cycles promote the lubrication and bonding weakening influence of water content on sandstone, which makes the migration of adsorption film on the surface of clay particles contained in sandstone and the slip between particles easier. Our experimental results were consistent with those obtained by scholars such as Liu et al. [23]. In addition, this test also used microscopic tests to combine the effects of freezing-thawing cycles, water content, and porosity. It was found that after freezing and thawing, the higher the water content of sandstone, the greater the porosity, which in turn led to the decline of its mechanical properties. In addition, this test also used microscopic tests to combine the effects of freezing-thawing cycles, water content, and porosity on sandstone. It was found that the higher the water content of sandstone after freezing and thawing, the greater the porosity, which in turn led to the decline of its mechanical properties.

In actual engineering, the rock mass usually bears three-dimensional load for a long time, rather than simply bearing the load in one direction. Future work should simulate the environment of the project site more realistically through triaxial compression test and creep test, further exploring the influence of freezing-thawing cycle times and water content on the creep characteristics of rock mass under long-term load.

7. Conclusion

(1) The stress-strain curves of sandstone with different water contents were roughly the same, mainly including the initial compaction stage, the elastic deformation stage, the plastic deformation stage, and the failure stage. However, the UCS and E of the sandstone decreased as the water content increased. The UCS and E decreased, respectively, by 37.31% and 25.05% when the water content increased by 2.80% from 0. The empirical equations used to describe the UCS and water content of sandstone, E, and water content were proposed.

(2) The SEM results showed that the number of micropores and microcracks in sandstone was increasing as the water content increased, leading to a gradual increase in plasticity. The porosity of dry sandstone to fully saturated sandstone was obtained by binarizing the SEM images, which increased from 3.56% to 10.36%. By analyzing the change law of UCS with water content and porosity, it was found that increasing water content led to increase in the porosity of sandstone under the freezing-thawing cycles. The increase in porosity was an important reason for the decline in the mechanical properties of sandstone. Additionally, the macroscopic failure form changed from splitting failure to shear failure.

(3) The AE ring count of sandstones with different water content varied roughly the same with time, showing that the ring count was small in the initial compaction and elastic stage, increased rapidly in the plastic deformation stage, and reached the maximum value in the failure stage. Various factors, such as water content, freezing-thawing cycles, and original cracks of the specimen, caused the relationship between AE ring count and water content to be insignificant.

Data Availability

The data used to support the findings of this study are available from the corresponding author upon request.

Conflicts of Interest

The authors declare that they have no conflicts of interest.

Authors' Contributions

Guilei Song, Longxiao Chen, and Kesheng Li contributed equally to this study.

Acknowledgments

We gratefully acknowledge the public service sector special funds from the National Natural Science Foundation of China (project no. 51574156) and the Key Development Program for Research of Shandong Province (project no. 2018GNC110023).

References

[1] M. Norikazu, "Mechanisms of rock breakdown by frost action: an experimental approach," *Matsuoka Norikazu*, vol. 17, no. 3, pp. 235–270, 1990.

[2] X. Fang, J. Xu, and P. Wang, "Compressive failure characteristics of yellow sandstone subjected to the coupling effects of chemical corrosion and repeated freezing and thawing," *Engineering Geology*, vol. 233, pp. 160–171, 2018.

[3] S. Z. S. Mousavi, H. Tavakoli, P. Moarefvand, and M. Rezaei, "Micro-structural, petro-graphical and mechanical studies of schist rocks under the freezing-thawing cycles," *Cold Regions Science and Technology*, vol. 174, Article ID 103039, 2020.

[4] S. Z. S. Mousavi, H. Tavakoli, P. Moarefvand, and M. Rezaei, "Assessing the effect of freezing-thawing cycles on the results of the triaxial compressive strength test for calc-schist rock," *International Journal of Rock Mechanics and Mining Sciences*, vol. 123, Article ID 104090, 2019.

[5] H. L. Jia, S. Ding, F. Zi, Y. H. Dong, and Y. J. Shen, "Evolution in sandstone pore structures with freeze-thaw cycling and interpretation of damage mechanisms in saturated porous rocks," *Catena*, vol. 195, Article ID 104915, 2020.

[6] H. Liu, Y. Wang, H. J. Wang, and Z. Q. Hou, "Experimental study on frost heaving pressure evolution of rock ice cracks under freezing-thawing cycles," *Journal of Engineering Geology*, 2019, https://kns.cnki.net/kcms/detail/11.3249.P.20200908.1139.007.html.

[7] Z. D. Su, J. Z. Sun, and J. Xia, "Experimental research of the effect of freezing-thawing cycles on acoustic emission characteristics of granite," *Chinese Journal of Rock Mechanics and Engineering*, vol. 38, no. 05, pp. 865–874, 2019.

[8] Y. Wang, J. Q. Han, and C. H. Li, "Acoustic emission and CT investigation on fracture evolution of granite containing two flaws subjected to freeze–thaw and cyclic uniaxial increasing-

amplitude loading conditions," *Construction and Building Materials*, vol. 260, Article ID 119769, 2020.

[9] H. B. Jiang, "The relationship between mechanical properties and gradual deterioration of microstructures of rock mass subject to freeze-thaw cycles," *Earth Sciences Research Journal*, vol. 22, no. 1, pp. 52–57, 2018.

[10] K. P. Zhou, B. Li, J. L. Li, H. W. Deng, and F. Bin, "Microscopic damage and dynamic mechanical properties of rock under freeze-thaw environment," *Transactions of Nonferrous Metals Society of China*, vol. 25, no. 04, pp. 1254–1261, 2015.

[11] L. Chen, K. Li, G. Song, D. Zhang, and C. Liu, "Effect of freeze-thaw cycle on physical and mechanical properties and damage characteristics of sandstone," *Scientific Reports*, vol. 11, no. 1, Article ID 12315, 2021.

[12] S. Huang, Q. Liu, A. Cheng, and Y. Liu, "A statistical damage constitutive model under freeze-thaw and loading for rock and its engineering application," *Cold Regions Science and Technology*, vol. 145, pp. 142–150, 2018.

[13] Y. Lu, X. Li, and A. Chan, "Damage constitutive model of single flaw sandstone under freeze-thaw and load," *Cold Regions Science and Technology*, vol. 159, pp. 20–28, 2019.

[14] J. Zhang, L. Miao, and Z. Yang, "Research on rock degradation and deterioration mechanisms and mechanical characteristics under cyclic freezing-thawing," *Chinese Journal of Rock Mechanics and Engineering*, vol. 27, pp. 1688–1694, 2008.

[15] M. H. Ghobadi, A. R. Taleb Beydokhti, M. R. Nikudel, A. Asiabanha, and M. Karakus, "The effect of freeze–thaw process on the physical and mechanical properties of tuff," *Environmental Earth Sciences*, vol. 75, no. 9, 2016.

[16] D. Wang, G. Chen, D. Jian, J. Zhu, and Z. Lin, "Shear creep behavior of red sandstone after freeze-thaw cycles considering different temperature ranges," *Bulletin of Engineering Geology and the Environment*, vol. 80, no. 3, pp. 2349–2366, 2021.

[17] J. L. Li, R. B. Kaunda, L. Y. Zhu, K. P. Zhou, and F. Gao, "Experimental study of the pore structure deterioration of sandstones under freeze-thaw cycles and chemical erosion," *Advances in Civil Engineering*, Article ID 9687843, 2019.

[18] Z. Zhou, X. Cai, W. Cao, X. Li, and C. Xiong, "Influence of water content on mechanical properties of rock in both saturation and drying processes," *Rock Mechanics and Rock Engineering*, vol. 49, no. 8, pp. 3009–3025, 2016.

[19] D. Li, L. N. Y. Wong, G. Liu, and X. Zhang, "Influence of water content and anisotropy on the strength and deformability of low porosity meta-sedimentary rocks under triaxial compression," *Engineering Geology*, vol. 126, pp. 46–66, 2012.

[20] Y. Lu, L. Wang, X. Sun, and J. Wang, "Experimental study of the influence of water and temperature on the mechanical behavior of mudstone and sandstone," *Bulletin of Engineering Geology and the Environment*, vol. 76, no. 2, pp. 645–660, 2017.

[21] Y. L. Liu and L. Li, "Failure characteristics underlying uniaxial compression of sandstone with different water content," *Journal of Heilongjiang University of Science and Technology*, vol. 30, no. 03, pp. 238–242, 2020.

[22] T. C. Chen, M. R. Yeung, and N. Mori, "Effect of water saturation on deterioration of welded tuff due to freeze-thaw action," *Cold Regions Science and Technology*, vol. 38, no. 02, pp. 127–136, 2003.

[23] Y. Liu, Y. Cai, S. Huang, Y. Guo, and G. Liu, "Effect of water saturation on uniaxial compressive strength and damage degree of clay-bearing sandstone under freeze-thaw," *Bulletin of Engineering Geology and the Environment*, vol. 79, no. 4, pp. 2021–2036, 2019.

[24] A. A. Omari, K. Beck, X. Brunetaud, Á. Török, and M. A. Mukhtar, "Critical degree of saturation: a control factor of freeze-thaw damage of porous limestones at Castle of Chambord, France," *Engineering Geology*, vol. 185, pp. 71–80, 2015.

[25] C. Walbert, J. Eslami, A. L. Beaucour, A. Bourges, and A. Noumowe, "Evolution of the mechanical behaviour of limestone subjected to freeze-thaw cycles," *Environmental Earth Sciences*, vol. 74, no. 7, pp. 6339–6351, 2015.

[26] L. F. Fan, C. Xu, and Z. J. Wu, "Effects of cyclic freezing and thawing on the mechanical behavior of dried and saturated sandstone," *Bulletin of Engineering Geology and the Environment*, vol. 79, no. 02, pp. 755–765, 2020.

[27] L. Weng, Z. Wu, A. Taheri, Q. Liu, and H. Lu, "Deterioration of dynamic mechanical properties of granite due to freeze-thaw weathering: considering the effects of moisture conditions," *Cold Regions Science and Technology*, vol. 176, Article ID 103092, 2020.

[28] K. S. Li, M. T. Li, D. Zhang, C. X. Liu, and D. P. Ma, "Effect of moisture content on bursting liability of sandstone due to freeze-thaw action," *Shock and Vibration*, vol. 2020, Article ID 8832528, 10 pages, 2020.

[29] ASTM D5312, "Standard test method for evaluation of durability of rock for erosion control under freezing and thawing conditions," *ASTM Standards*, vol. 12, no. 6, 2013.

[30] Ministry of Water Resources of the People's Republic of China, *SL264-2001, Specifications for Rock Tests in Water Conservancy and Hydroelectric Power Engineering*, China Water & Power Press, Beijing, China, 2001.

[31] S. P. Ding, *Experimental Study on Deformation and Failure Change of sandstone under Freeze-Thaw Cycles*, Liaoning Technical University, Fuxin, China, 2019.

[32] J. D. Jiang, S. S. Chen, J. Xu, and Q. S. Liu, "Mechanical properties and energy characteristics of mudstone under different containing moisture states," *Journal of China Coal Society*, vol. 43, no. 08, pp. 2217–2224, 2018.

[33] X. Wang, Z. Wen, Y. Jiang, and H. Huang, "Experimental study on mechanical and acoustic emission characteristics of rock-like material under non-uniformly distributed loads," *Rock Mechanics and Rock Engineering*, vol. 51, no. 3, pp. 729–745, 2018.

[34] D. Ma and Y. Zhou, "Creep behavior and acoustic emission characteristics of coal samples with different moisture content," *Acta Geodynamica et Geomaterialia*, vol. 15, pp. 405–412, 2018.

[35] H. Qin, G. Huang, and W. Z. Wang, "Experimental study of acoustic emission characteristics of coal samples with different moisture contents in process of compression deformation and failure," *Chinese Journal of Rock Mechanics and Engineering*, vol. 31, no. 06, pp. 1115–1120, 2012.

[36] Z. Zhou, X. Cai, D. Ma, W. Cao, L. Chen, and J. Zhou, "Effects of water content on fracture and mechanical behavior of sandstone with a low clay mineral content," *Engineering Fracture Mechanics*, vol. 193, pp. 47–65, 2018.

[37] C. J. Chen, Y. J. Zhao, S. L. Guo, L. Zhao, and Y. T. Pan, "Experimental study on acoustic emission characteristics of coal with different moisture content," *Safety In Coal Mines*, vol. 49, no. 5, 2018.

[38] D. C. Jiang, W. S. Yang, and H. Bai, "Experimental study of the effects of moisture content on the mechanical properties of sandstone under uniaxial compression," *IOP Conference Series: Earth and Environmental Science*, vol. 768, no. 1, Article ID 012017, 2021.

[39] S. Huang, Y. He, G. Liu, Z. Lu, and Z. Xin, "Effect of water content on the mechanical properties and deformation characteristics of the clay-bearing red sandstone," *Bulletin of Engineering Geology and the Environment*, vol. 80, no. 2, pp. 1767–1790, 2021.